X. ENERGY CONVERSION RESEARCH*

Academic and Research Staff

Prof. G. A. Brown
Prof. E. S. Pierson
Prof. J. L. Kerrebrock
Prof. M. A. Hoffman
Prof. C. C. Oates
Prof. J. E. McCune

Graduate Students

E. K. Levy
R. J. Thome
R. Decher
G. W. Zeiders, Jr.
W. H. Evers, Jr.

A. A LARGE NONEQUILIBRIUM MHD GENERATOR

1. Introduction

It has been clear for some time that nonequilibrium ionization caused by electron heating can be produced in magnetogasdynamic generators, provided the Joule dissipation in the gas can be raised to the level required to elevate the electron temperature.[1,2] Idealized generator calculations predict that it should be quite easy to realize such levels of dissipation. In practice, however, generators operating with the seeded noble gases, which seem optimum for production of electron heating, have, for the most part, failed to yield the expected nonequilibrium ionization. The outstanding exception to this statement is the disc-type Hall generator described by Klepeis and Rosa.[3] The data supporting these conclusions has been summarized by Kerrebrock.[4]

It has been proposed by one of the present authors that the lack of success of the segmented-electrode generators can be attributed to a shorting of the Hall field by a highly conducting layer of gas near the electrode wall.[5] It was proposed that the high conductivity initially results from the concentrated dissipation resulting from the electrode segmentation and is supported by the dissipation caused by the shorted Hall current. The theory appears to explain the behavior of a least two generators, one of which operated at a low Hall parameter, for which the shorting effect was predicted to be small, and the other at a high Hall parameter, for which the effect should be very large.

The success of the disc-type Hall generator is further evidence in support of the theory, since the losses attributable to electrode segmentation are eliminated in this design.

It might then seem that the disc geometry is optimum for nonequilibrium generators. But, since this is a Hall generator, this type suffers from the disadvantage that it must operate at very large Hall parameters in order to yield the levels of efficiency desired for nuclear-MHD power plants. At these large Hall parameters, other losses, such as

*This work was supported by the U. S. Air Force (Research and Technology Division) under Contract AF33(615)-3489 with the Air Force Aero Propulsion Laboratory, Wright-Patterson Air Force Base, Ohio.

those that are due to electrothermal waves[6,7] and steady nonuniformities,[8] may seriously degrade the efficiency.

For these reasons, a systematic attempt has been made to design a segmented-electrode generator which will not exhibit the electrode shorting phenomenon and still be capable of elevation of the electron temperature above the gas stagnation temperature. The design has been based on the results of the theory given elsewhere.[5] It will be described in detail below.

We were fortunate in having available for the study a graphite inert-gas heater capable of a flow of 0.4 kg s^{-1} of helium at 2000°K stagnation temperature and 5 atm stagnation pressure. This makes possible a supersonic flow in which viscous effects are small.

As we shall see, the results of the experiments conducted thus far do not prove the engineering feasibility of segmented electrode nonequilibrium generators. They do serve, however, to indicate some of the critical problems remaining to be solved.

2. Description of the Facility

The hot plasma for use in the experiments is supplied by a large heat-sink facility illustrated in Fig. X-1. This facility is similar in concept to the conventional pebble-bed heaters, but here the core is constructed of 7 separate cylindrical blocks of graphite, 22 inches in diameter, each of which is drilled with approximately 1100 1/4 inch holes. The core is heated electrically by graphite glow bars at an input power of approximately 250 kilowatts. Thermal insulation is provided by graphite felt and graphite fibres. Electrical insulation is provided by boron-nitride spacers.

The test gas is supplied from a manifold of up to 20 gas bottles, and is delivered through two stages of regulators in series, to the inlet at the bottom of the heater. The seed material is injected by a motor-driven stainless-steel syringe into a "bed" of oxygen-free copper bars which have been heated to 1100°K. A subsidiary flow of the flow of the test gas is also passed through the copper bars, and the mixture of vaporized seed material and gas is injected into the plenum chamber at the outlet from the graphite core, where it mixes with the mainstream. The seed is carried from the copper bed to the plenum by a molybdenum tube sheathed with graphite.

No serious problems have been encountered in repeated operation of this facility at 2000°K. This temperature is the approximate limit set by the balance of the available input power against the heat losses.

3. Description of the Channel

a. Over-all Channel Geometry

The MHD channel over-all dimensions were selected to take maximum advantage of the magnet that was used. The magnet has pole face dimensions of 6 × 18 inches and

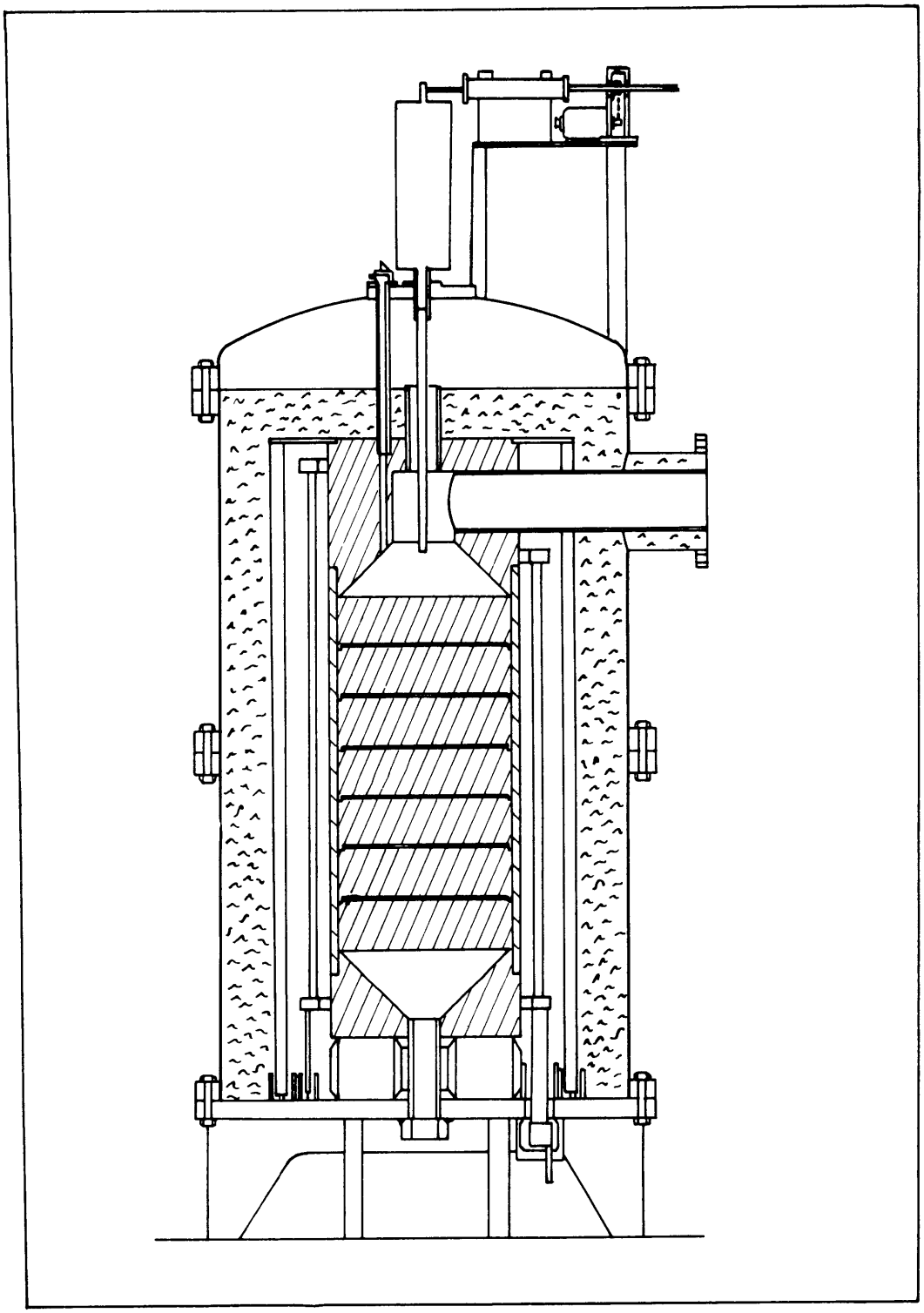

Fig. X-1. Inert-gas heater facility.

produces approximately 1.3 Tesla at a gap of 2 1/4 inches. As a result, an MHD channel with a length of 18 inches and an exit height of 6 inches was selected (see Figs. X-2, X-3, X-4, X-5).

The channel was designed for the following nominal flow conditions: inlet Mach number of 2.0 with inlet stagnation temperature of 2000°K, inlet stagnation pressure of 5 atm and mass flow of helium of 0.40 kg/sec. This led to the over-all dimensions shown in Fig. X-2.

A water-cooled copper nozzle of rectangular cross section and constant width was designed and built to provide the desired inlet Mach number to the channel with a smooth transition. This nozzle was effectively at ground potential.

A rectangular, constant-area supersonic diffuser was designed to provide good pressure recovery. Great care was exercised in the design to insure electrical isolation of the MHD channel and plasma from ground. The diffuser walls consist of small copper bricks or blocks 1 1/2 × 1/2 inches deep mounted on an epoxy plastic support wall. The blocks have sufficient volume to remain at low temperature throughout the run, since the run duration is short. Also, each block is electrically and thermally insulated from adjacent blocks and from the support wall by mica strips, 1/16 inch thick.

A copper subsonic diffuser was attached to the exit of the supersonic diffuser. The plasma exhausted into a large plenum chamber vented to atmospheric pressure. This plenum was electrically insulated from ground.

b. Electrode-Wall Design

The electrode geometry and materials were selected on the basis of the theory previously developed[5] for the behavior of segmented electrodes in a generator where nonequilibrium ionization of the gas is possible. In order to suppress the electrode-wall shorting predicted by this theory, it is desirable to use rather coarse segmentation ratios (i.e., the ratio of the channel height to electrode pitch) of the order of 5 to 10. The theory also indicates that it is advantageous to keep the electrode wall cold in order to suppress the nonequilibrium ionization in the gas layer near that wall.

An electrode pitch of 3/4 inch was selected. This yields a segmentation ratio of 4.7 at the inlet increasing to 8.0 at the channel exit.

As shown in Fig. X-2, the electrode itself is made of pyrolytic graphite, 5/16 inch long and 1 1/2 inches wide. The laminae of the pyrolytic graphite lie parallel to the electrode-wall surface in order to promote heating of the emitting surface of the electrode and reduce heat transfer into the electrode. Each electrode is mounted in a U-shaped copper yoke to which the external electrical connection is made.

Since the run durations were from 10 to 30 seconds, the heat-sink principle was employed in designing insulator segments that would remain cold throughout the run. These consisted of copper blocks of sufficient volume to remain at low temperatures

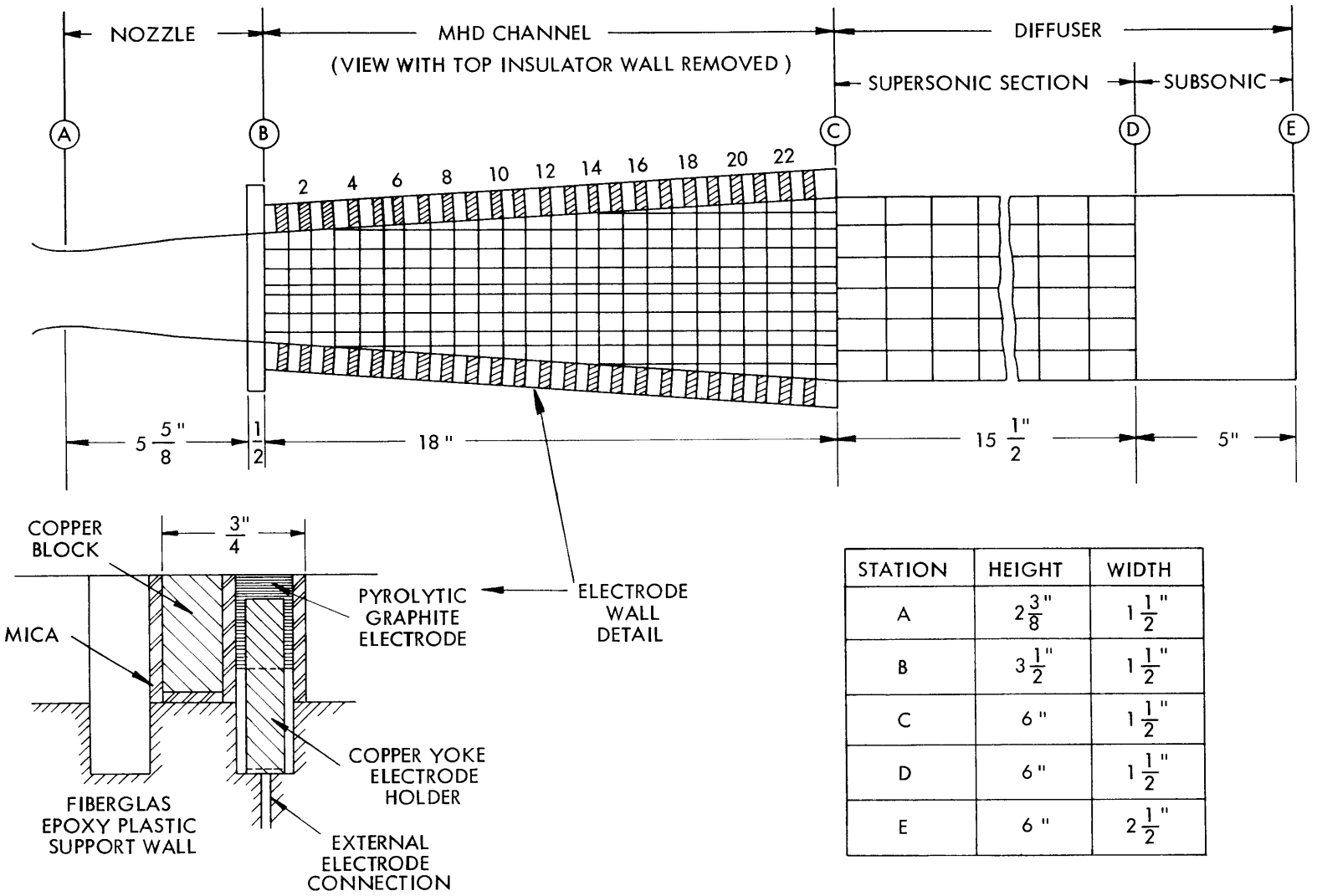

STATION	HEIGHT	WIDTH
A	2 3/8"	1 1/2"
B	3 1/2"	1 1/2"
C	6"	1 1/2"
D	6"	1 1/2"
E	6"	2 1/2"

Fig. X-2. MHD channel layout.

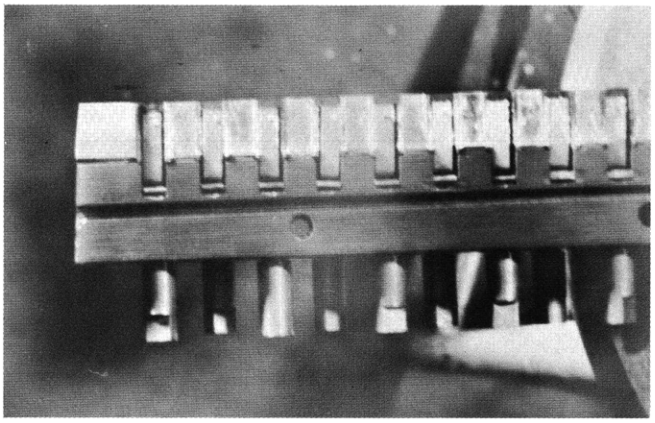

Fig. X-3.

Side view of electrode wall showing first nine segmented electrodes.

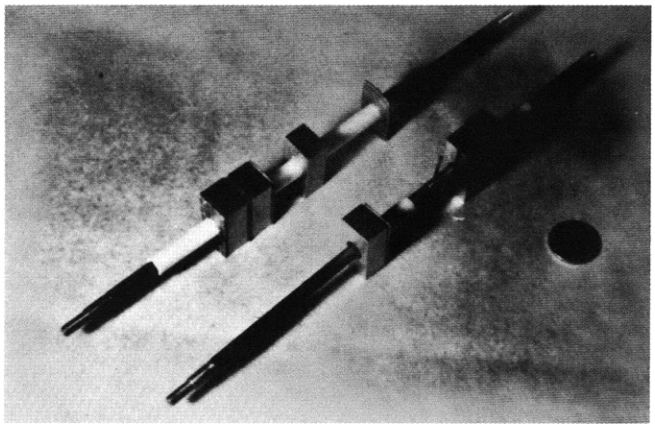

Fig. X-4.

Assembly of Armco iron blocks for insulator wall on steel bolts covered with mica tubes.

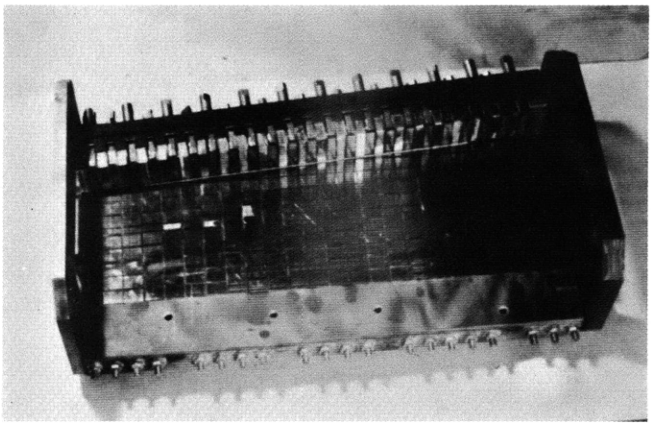

Fig. X-5.

MHD channel partly assembled showing top electrode wall mounted on insulator wall.

(≈200°C) for the expected test durations. These copper blocks were electrically and thermally insulated from the adjacent electrodes and the support wall by mica strips, 1/16 inch thick.

Twenty-three electrodes and insulator segments were assembled on each Fiberglas epoxy plastic-support wall.

c. Insulator-Wall Design

The first insulator wall consisted of sheets of boron nitride, 1/4 inch thick, epoxied to a plastic-support wall. As will be discussed below, insulator wall and/or insulator boundary layer shorting revealed by the results of runs 1 and 2 led to redesign of this wall.

The second insulator wall was assembled from small blocks of Armco magnet iron, each of which was electrically and thermally insulated by thick mica strips, 1/16 inch thick, similarly to the diffuser-wall design. The iron blocks had sufficient depth to remain at relatively low temperature during the run. The use of iron reduced the effective magnet gap to a minimum and increased the magnetic field to 1.4 Tesla.

Each set of blocks lying in the transverse direction was assembled on a long bolt covered with a mica tube for electrical insulation. Holes were drilled along the axis of each bolt and a small pressure tap was inserted into each bolt between two iron blocks. These flush-wall static pressure taps on the insulator wall provided a detailed profile of the static pressure in the flow direction.

The sets of iron blocks were assembled on epoxy plastic-support walls which also provided a pressure-tight seal for the entire insulator wall.

d. Exciter

In order to examine the effect of higher electron density on the starting characteristics of the generator, an external exciter was designed and installed at the entrance of the channel. Several different configurations were used in the various runs. In all cases, a battery bank was used to apply a DC voltage across the channel near the entrance. This battery bank was so connected that it could be inserted or removed when desired during the run at each test condition. In all runs, data were taken at a series of load resistances both with the exciter batteries connected and removed.

In run 2, a 360-volt battery bank was connected across electrode pairs 1, 2, and 3. There was provision for inserting this exciter voltage in series with the load resistor when desired.

In runs 3 to 6, the battery bank was connected only to electrode pair 3. Electrodes 1 and 2 were left open throughout the run. The voltage applied in runs 3, 5, and 6 was 260 volts. In run 4, this voltage was reduced to ~75 volts. In run 6, a 3-ohm resistor was permanently connected across electrode pair 3 throughout the run. As in all other

runs, the exciter batteries could be inserted in series with the load resistor when desired.

The exciter was removed from the electrodes altogether in runs 7 and 8 and connected to the row of insulator wall blocks near electrode pair 2. In run 7, a set of four 12-volt batteries was connected across each of the 7 pairs of insulator wall blocks through a 4-ohm external resistor. These batteries could be applied across the channel so that the current would flow in the direction of the magnetic field. In run 8, a battery bank totaling 260 volts was connected across all 7 pairs of iron blocks with the blocks in parallel.

4. Experimental Results

Eight experimental runs have been conducted thus far, two with the boron-nitride side walls, and six with the iron-peg walls. Of these, the most useful were runs 2, 5, 6, and 7. The principal parameters for these are listed in Table X-1. Helium seeded with cesium was used as working gas in all of the listed runs.

Table X-1. Parameters for experimental runs.

Run No.	Side Wall	P_s (atm)	Cs Mole Fraction	Hall Parameter	T_s (°K)	M	p (atm)	B (Tesla)
2	BN	4.5	.002	3.8	2000	2.1	.50	1.3
5	Iron	4.1	≈0	4.5-6.3	2000	2.1-2.5	.45-.27	1.4
6	Iron	3.1	.003	6.0-8.3	2000	2.1-2.5	.34-.21	1.4
7	Iron	4.5	.002	4.1-5.7	2000	2.1-2.5	.50-.30	1.4

It should be noted at the outset that in none of the runs did the generator produce a significant fraction of the expected power. The data have not been completely analyzed so it will be possible to report only the experimental results, and offer some possible reasons for the poor performance of the generator.

From the pressure distributions (see Fig. X-6), we conclude that the channel operated supersonically, and essentially at the design Mach numbers of 2 at the inlet and 2.5 at the outlet in all runs in which the stagnation pressure was above ~3 atm absolute. As will be noted below, there is a possibility that the magnetogasdynamic effects led to separation on the cathode wall.

The iron-peg-wall channel was operated with a mixture of 70 per cent Argon, 30 per cent Helium, as a Faraday generator in run 3 and as a Hall generator in run 4. In both

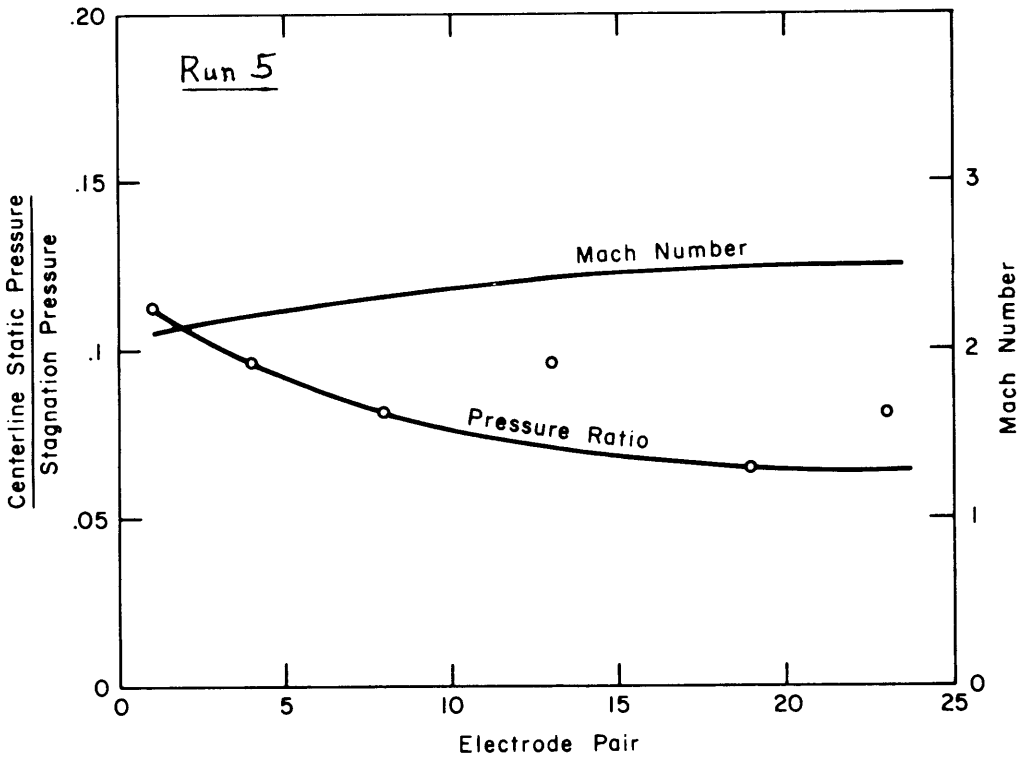

Fig. X-6. Typical static pressure and Mach number variations along the channel.

cases, the open-circuit coltages were very low, and the output negligible. Although the reasons for this are not fully understood, it is probable that the higher Hall parameter and lower electrode temperatures were major contributing factors.

a. Boron-Nitride Side-Wall Runs

The channel with boron-nitride side walls was operated at the test conditions given for run 2 in Table X-1. For these conditions, as for the remaining runs, the conductivity of the plasma should have been approximately 5 mho m^{-1} if the electron mole fraction were frozen at the stagnation value.

An attempt was made to start the generator by applying a potential to electrode pairs 1, 2, and 3 so as to increase the current in these electrode pairs. With the exciter operating, the currents indicated in Fig. X-7 were produced. It will be noted that the current per electrode pair increased down the channel, more rapidly with the 3-ohm load resistance than with the 10-ohm and 25-ohm resistors. From this it may be inferred that the conductivity was increasing down the channel.

The voltage-current characteristics for electrode pairs 5 and 23 are compared (see Fig. X-8) to the characteristic that would be expected for ionization frozen at the stagnation value, and with electrode losses characteristic of the "normal mode."[5] This

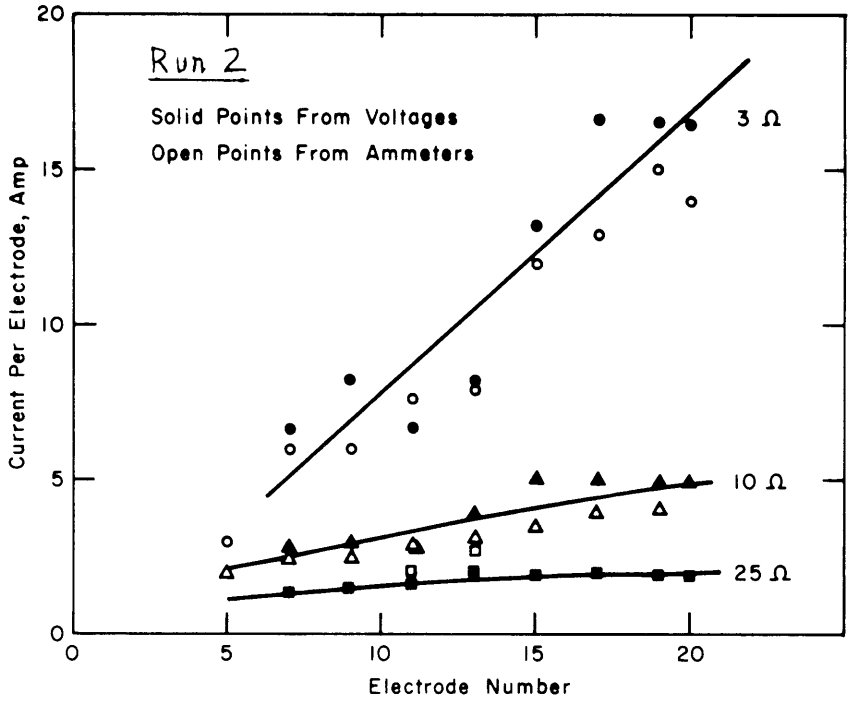

Fig. X-7. Current per electrode pair along the channel for various load resistances.

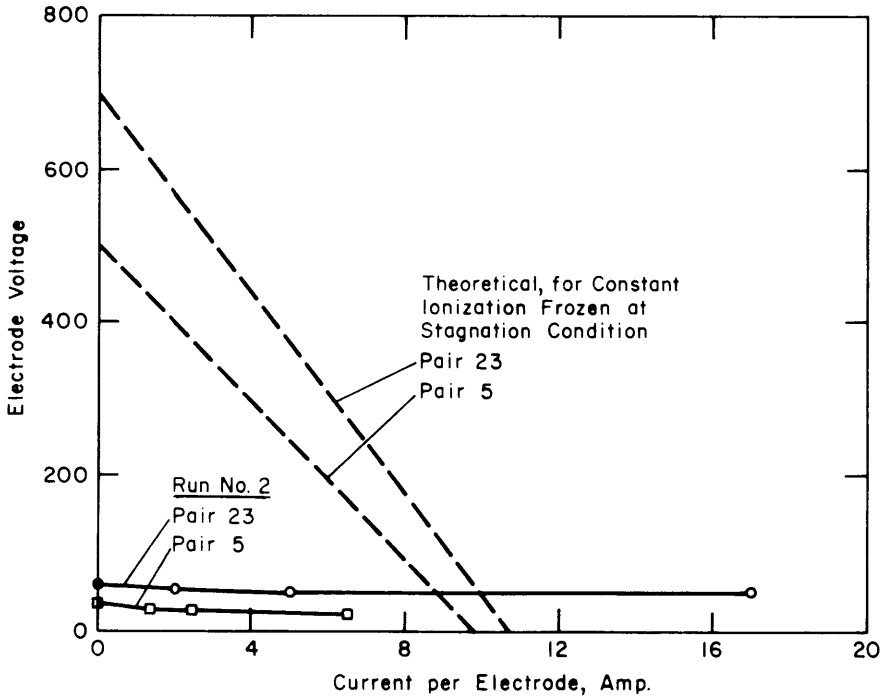

Fig. X-8. Voltage-current characteristics for two representative electrode pairs.

performance is nearly equal to that predicted by the electrode theory of Hurwitz, Kilb, and Sutton,[9] and seems to be a reasonable upper limit to what can be expected if no electron heating occurs.

We see that the open-circuit voltage was very much less than the expected value; however, the current in electrode pair 23 did exceed the frozen ionization value by a substantial factor.

When the exciter was turned off, the currents were negligible.

From the low open-circuit voltage, it was concluded that the generator was probably internally shorted through the boundary layer on the insulating wall. Because of its low thermal conductivity, the boron-nitride side wall ran quite hot, and it was felt that this probably aggravated the shorting.

Accordingly, the iron side walls described above were constructed.

b. Iron Side-Wall Runs

In run 5, the generator was operated with very low seed fraction (because the seeder jammed), both with and without excitation on electrode pair 3. The exciter made very little difference in this run, so the data will be given for points without excitation.

More detailed instrumentation was available for this channel than for the previous one, so that it has been possible to prepare the approximate potential diagrams shown

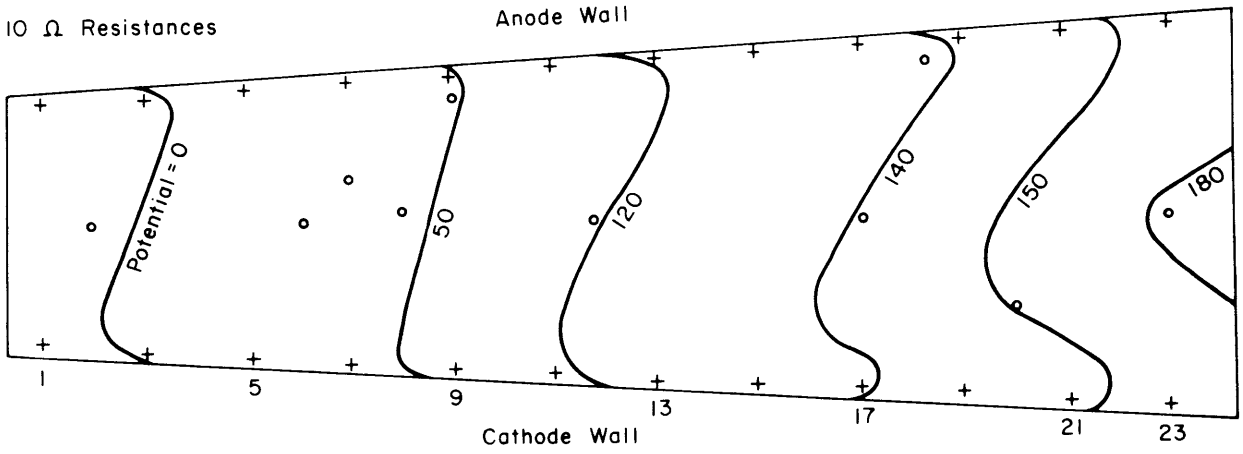

Fig. X-9. Approximate potential diagram for 10-ohm load resistances for run 5.

in Figs. X-8, X-9, and X-10. The crosses indicate points where the voltage was measured at the electrodes, while the circles indicate probes on the insulating wall.

A representative potential diagram from run 5 for the 10-ohm load case is shown in Fig. X-9. The potential pattern is almost symmetric but does show some evidence of a potential "valley" along the cathode wall. This region of low potential tended to

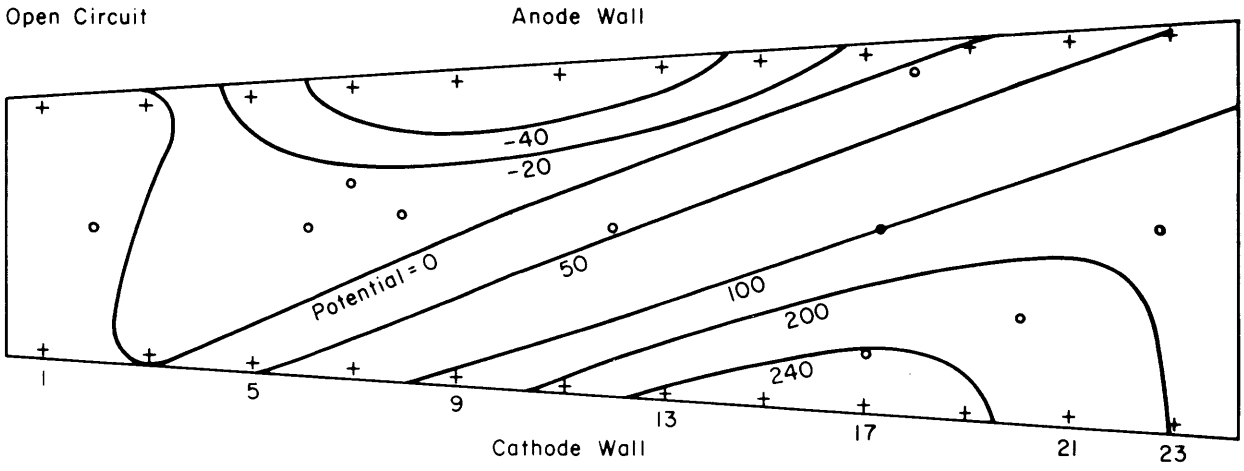

Fig. X-10. Approximate potential diagrams for open-circuit condition for run 6.

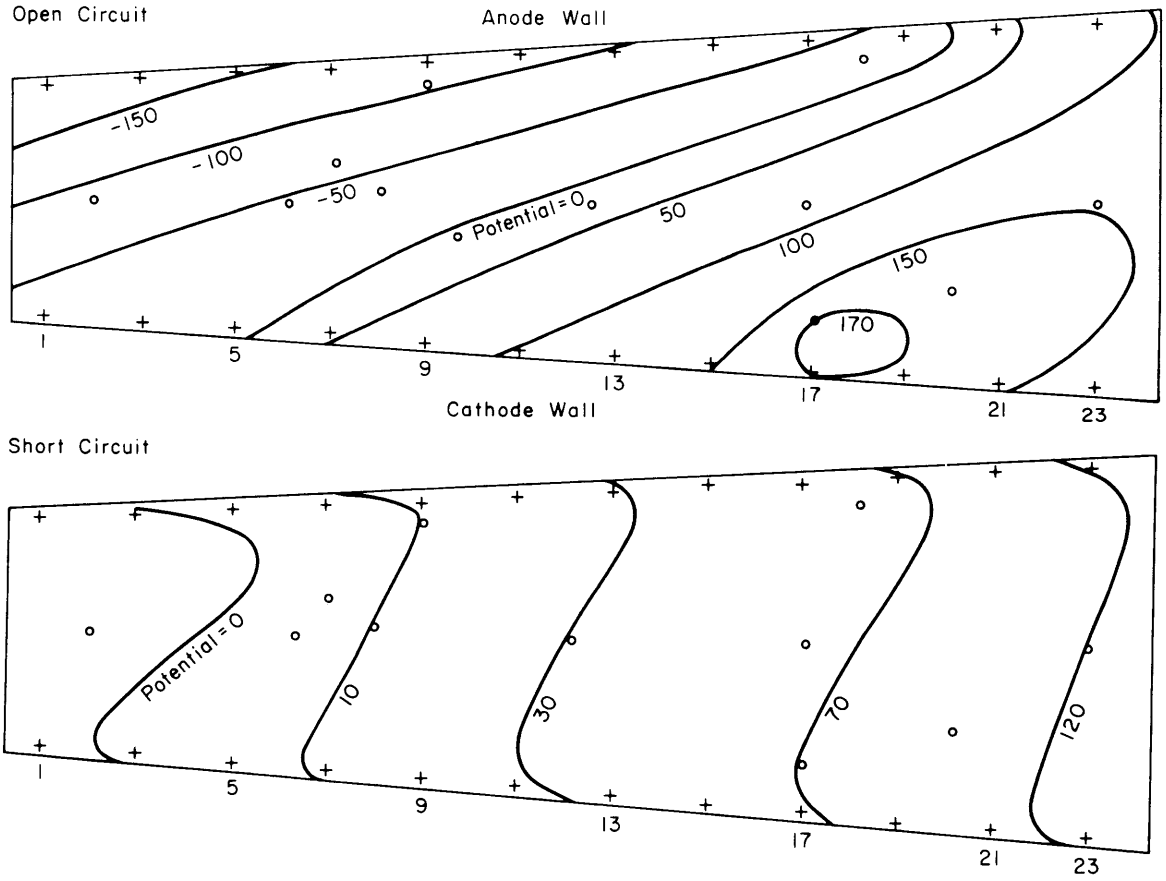

Fig. X-11. Approximate potential diagrams for open-circuit and short-circuit conditions for run 7.

grow at larger load resistances. At lower load resistances it tended to diminish, and essentially disappeared at short circuit.

In run 6, the same channel was operated at a relatively low stagnation pressure, and high seed fraction. The Hall parameter varied between 6.0 at the channel entrance and 8.3 at the exit. A 3-ohm load was maintained on electrode pair 3 for all points. With these conditions, an open-circuit voltage of 365 volts was produced at electrode pair 15. The approximate potential diagram for the open-circuit is shown in condition Fig. X-10. When a load was applied, the channel behaved much as in run 5.

Run 7 was made with almost the same gas conditions as in run 2; data for the cases without excitation are presented. The potential plots for open circuit and short circuit are given in Fig. X-11. Two open-circuit points were taken, one at the beginning of the run and one at the end. At the beginning of the run, the open-circuit voltage reached a maximum of only 75 volts, compared with the 250 volts of Fig. X-11.

Again, the trends are as in runs 5 and 6, with a potential minimum along the cathode wall at open circuit, and large potential drops along both electrodes at short circuit.

5. Discussion of Results

From the potential diagrams, one can construct an approximate current pattern in the channel. We note first that Ohm's law can be written in the form

$$\sigma\vec{E}' = \vec{j} + \beta\frac{\vec{j} \times \vec{B}}{B},$$

where σ is the scalar conductivity, β is the Hall parameter, and $\vec{E}' = \vec{E} + \vec{u} \times \vec{B}$ is the electric field in the gas. Thus, $\vec{j}$ flows at the angle $\tan^{-1}\beta$ to $\vec{E}'$.

Consider first the short-circuit condition for run 7. The directions of $\vec{E}$, $\vec{E}'$, and $\vec{j}$ in the free stream and at the electrode wall are as shown schematically in Fig. X-12a. There is a large Hall current flowing downstream in both locations, while the transverse current flows from anode to cathode, as expected. As the load resistances were decreased, the component of current normal to the electrodes increased, as deduced from rotation of the potential lines so as to be more nearly perpendicular to the axis.

At the surface of the insulator wall, the current flows at the angle $\tan^{-1}\beta$ to the direction of $\vec{E}$, since $\vec{u}$ is small. Thus, the Hall current component reverses and flows upstream. This strongly suggests that the poor performance of the generator in the loaded configuration is due to an axial short of the Hall potential through the boundary layer along the insulating wall.

Next, consider the open-circuit condition for run 7. The current diagram for this case is Fig. X-12b. In the free stream, the current flows more nearly along the axis, as would be expected. At the insulator wall, its Hall component is reversed as before.

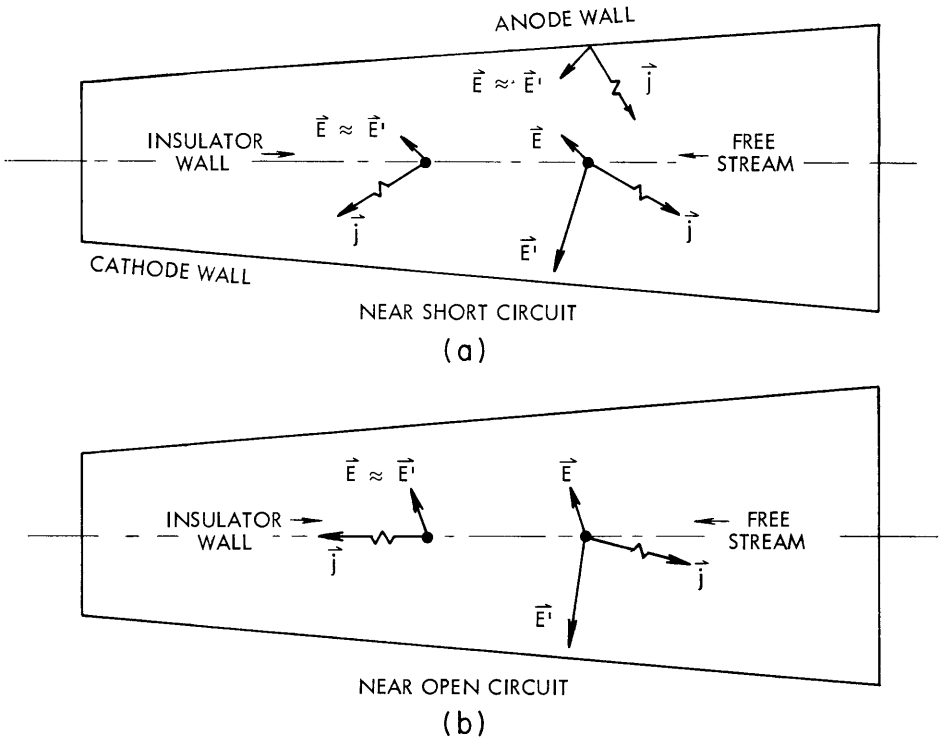

Fig. X-12. Schematic diagram of electric fields and currents for short-circuit and open-circuit conditions in run 7.

The transverse component may also reverse if the open-circuit voltage is large enough. To the accuracy that the current diagrams can be drawn, it is difficult to determine whether the transverse current is positive or negative at this point.

The low-potential region near the cathode has the appearance of a separated region, as reported by Louis, Gal, and Blackburn.[10] Such a separation is consistent with a very large Hall current in the free stream, since such a current would produce a $\vec{j} \times \vec{B}$ force toward the cathode. Such a large Hall current, however, would have to be supported by a large transverse current. The return path for this transverse current is not clear, at present. It may be through the insulator boundary layer.

6. Conclusions

On the basis of these preliminary results, we conclude that the behavior of the insulator boundary layer is a crucial factor in determining the performance of supersonic inert-gas generators. There seems to be no evidence in the present results that the electrode shorting phenomenon previously described[5] limited the performance of these generators.

J. L. Kerrebrock, M. A. Hoffman, G. C. Oates, R. Decher

References

1. J. L. Kerrebrock, "Conduction in Gases with Elevated Electron Temperatures," Engineering Aspects of Magnetohydrodynamics (Columbia University Press, New York, 1962), pp. 327-346.
2. J. L. Kerrebrock and M. A. Hoffman, "Nonequilibrium Ionization Due to Electron Heating: II. Experiments," AIAA J. 2, 1080-1087 (1964).
3. J. Klepeis and R. J. Rosa, "Experimental Studies of Strong Hall Effects and V X B Induced Ionization," Fifth Symposium on Engineering Aspects of Magnetohydrodynamics, Massachusetts Institute of Technology, Cambridge, Massachusetts, April 1964.
4. J. L. Kerrebrock, "Magnetohydrodynamic Generators with Nonequilibrium Ionization," AIAA J. 3, 591-601 (1965).
5. J. L. Kerrebrock, "Segmented Electrode Losses in MHD Generators with Nonequilibrium Ionization-II," Avco-Everett Research Report 201, January 1965.
6. J. L. Kerrebrock, "Nonequilibrium Ionization Due to Electron Heating: I. Theory," AIAA J. 2, 1072-1080 (1964).
7. R. Dethlefsen and J. L. Kerrebrock, "Experimental Investigation of Fluctuations in a Nonequilibrium MHD Plasma," Seventh Symposium on Engineering Aspects of Magnetohydrodynamics, Princeton University, Princeton, New Jersey, 1966, pp. 117-125.
8. R. J. Rosa, "Hall and Ion-Slip Effects in a Nonuniform Gas," Phys.Fluids 5, 1081-1090 (1962).
9. H. Hurwitz Jr., R. W. Kilb, and G. W. Sutton, "Influence of Tensor Conductivity on Current Distribution in an MHD Generator," J. Appl. Phys. 32, 205 (1961).
10. J. F. Louis, G. Gal, and P. R. Blackburn, "Detailed Theoretical and Experimental Study on a Large MHD Generator," AIAA J. 3, 1482-1490 (1965).